CONTROLLED-STRAIN RATE TESTS AT VERY LOW STRAIN RATES OF 2618 ALUMINUM AT 200°C

J.L. Ding, S.R. Lee
Department of Mechanical Engineering
Washington State University
Pullman, Washington 99164-2920

Constant strain rate tests and constant load creep tests were performed on 2618 aluminum at 200°C. The strain rates used in the constant strain rate tests were 10^{-6}, 10^{-7}, 10^{-8}, and 10^{-9}/sec. Due to the fact that the strain rates in both tests were comparable to each other, the similarities between them can therefore be studied.

It was concluded that metals are essentially rate sensitive at elevated temperatures. The traditional definition of creep and plasticity used in the classical creep analysis is actually a reflection of the material behavior under different loading conditions. A constitutive equation based on the test data under one loading condition should work well for other loading conditions as long as the strain rates are in the same range as those under which the material constants are determined.

Introduction

Classically the constitutive equations used in the design of components of fast breeder reactor (FBR) or pressure vessels are mostly based on the idea that the total strain can be decomposed into elastic strain, plastic strain, creep strain, and thermal strain (1). The elastic strain and the plastic strain are defined as the instantaneous response to stress change which is time-independent, while the creep strain is defined as the time-dependent strain under constant load. The constitutive equations for the plastic strain component are based on the classical rate-independent plasticity theory in which the concept of yield surface plays a very important role; and those for the creep strain component are generally based on strain-hardening viscous flow rule which, in most of the cases, needs to be modified in order to incorporate the anisotropy induced by deformation (2). Since the inelastic strain is decomposed into plastic strain and creep strain, there have also been some followup studies on the interaction between creep and plasticity (3).

The new trend in modelling the inelastic material behavior, however, is toward a unified approach in which the traditional creep and plasticity are treated by a unified equation. This approach is reasonable based on the fact that both creep strain and plastic strain are contributed mainly by the same deformation mechanism, i.e., dislocation motion. On the other hand, the way to distinguish creep strain from plastic strain in the traditional approach is also somewhat too arbitrary. It is actually based on the way the material is tested. For example, in the study of creep-plasticity interaction, the material testing usually started with a constant strain rate loading followed by a period of constant-load loading, or vice versa. The inelatic strain accumulated during constant strain rate loading is considered as plastic strain, while the strain accumulated during the constant load period is treated as creep strain. This definition probably follows the tradition that plasticity is usually studied with constant strain rate tests, while creep is studied with the constant load test.

In the current study, both constant strain-rate tests and creep tests were performed on 2618 aluminum alloy. The strain rates adopted were in the range from 10^{-9}/sec to 10^{-6}/sec. The simularities between these two tests were investigated. The purposes of this study are:

1) To justify the unified theory for creep and plasticity.
2) To study the concept of creep-plasticity interaction.
3) To compare the steady state response of engineering materials under constant-strain rate loadings with that under constant-load loadings.

In addition, one test under combined tension and torsion loadings was also performed to study the effects of shear stress on the axial stress-strain relation at constant strain rate.

Material and Specimen

The material employed in the present work was aluminum forging alloy 2618-T61 which was the same kind of material as that used in previous work (4-7), but obtained three years later from the same source, probably from a different batch. The heat treatment was carried out at different place too. Some variations in the mechanical properties were found between these two

batches. However, since previous work were not referred in the current study, these variations may be disregarded.

Specimens were thin-walled tubes of circular cross section. The nominal outside diameter, wall thickness, and gage length were 25.4, 1.5, and 101.6 mm respectively.

Experimental Apparatus

All the tests were performed with a combined tension and torsion creep machine whose details can be found in the paper by Findley and Gjelsvik (8). The relative axial displacement between the gage points was measured by a matched pair of linear variable differential transformers (LVDT) using an AC-null balance system. One LVDT was attached to the gage points through four invar rods and the other (reference LVDT) was connected to a micrometer. Before the test, the outputs of these two LVDT's cancelled each other, i.e., balanced. During the test some imbalance was induced, due to the relative displacement between the gage points, which would be balanced out again with the reference LVDT by turning the micrometer. The relative displacement could then be read from the micrometer.

In order to use the current machine to perform controlled strain-rate tests, some modificiations were necessary. The desired strain rates were obtained by use of several AC reversible synchronous motors to drive the reference LVDT at specified speeds and an servohydraulic system to apply the load in such a way that the output from the LVDT attached to the specimen always matches with that of the reference LVDT, i.e., the specimen is stretched at a speed determined by the motor. Unlike the tests done in a conventional tensile testing machine with constant "crosshead" speed, the current tests are truly strain rate controlled tests because the servo-hydraulic system is driven directly by the output from the extensometer.

The specimen was heated internally by a quartz-tube, radiant heating lamp and externally by two resistance heaters at the ends just outside the gage length. The lamp and the end heaters were controlled separately by two sets of Research Incorporated temperature controller and power controller. The test temperature was 200°C. Prior to testing, the specimen was soaked at the testing temperature for approximately 18 hours. The details of the choice of 18 hours as the soaking time can be found in the paper by Ding and Findley (7).

Experimental Results

The experimental results are shown in the attached figures. In figure 1(b) the solid line is the test data on the stress-strain relation for a controlled-strain-rate test under stepwise increased strain rates, namely 1.04×10^{-8}/sec, 1.0×10^{-7}/sec, and 1.0×10^{-6}/sec followed by unloading at a strain rate of 1.04×10^{-8}/sec as shown in figure 1(a). Figure 2 is another controlled strain rate test under stepwise decreased strain rates. For both tests, a steady state can be found for each particular strain rate in which the stress remains constant. The steady state stress at each step in figure 1(b) is lower than that in the corresponding step with the same strain rate in figure 2(b), respectively. This may be due to the different strain histories and strain rate histories involved in these two tests. In figure 1(b), it can also be seen that the slope during unloading is higher than that during loading. This may be explained as follows: during loading, the time-dependent strain is developed in the same direction as the imposed strain rate direction, while during unloading, they are opposite to each

other. Therefore, for the same imposed strain rate, less stress may be required during loading than during unloading. Similar observations can also be found in figure 2(b). However, loading and unloading were carried out at different strain rates in this test.

The creep test data under step loadings are shown in figure 3. The stress at each step was chosen the same as the steady state stress at the corresponding step in figure 1, namely, 172.5 MPa, 195 MPa, and 216 MPa, respectively. Similar to figure 1, a steady state was also found in each loading step. A comparison of the material responses between these two tests is shown in figure 4. The steady state responses at each step are quite close to each other. The deviation is within 10%. The major differences between these two tests seem mainly on the transient responses.

Shown in figure 5 are the test results of axial loading at constant strain rate combined with stepwise varied torsional loadings. The effect of shear stress on the ongoing axial material response to a constant-strain-rate loading can be clearly seen. It is quite interesting to notice that the combination of axial stress and shear stress at new steady state for steps 2, 3, and 4 satisfy the Tresca relation, i.e, $\sigma^2 + 4\tau^2 =$ constant, as shown in figure 5(c). However, the implication of this relation is not quite clear in this case. From figure 5(b), it can also be seen that the steady state axial stress in the later stage, i.e., when the shear stress is completely released, is lower than the initial steady state stress before the shear stress was applied. Similar observations can also be found for the two steps with the same shear stress, namely 55.6 MPa. This may indicate that some kind of softening may have occurred.

Discussion of the Experimental Results

In figure 6, the stress-strain curves at different strain rates discussed earlier were put together. As shown in this figure, a distinguishable elastic region can be found for each curve. The point at which the curve starts to deviate from the straight line may be defined as the so-called yield stress and the dependence of the yield stress on strain rate may be interpreted as the rate-sensitive yielding in the theory of viscoplasticity. From these results, the first conclusion we may draw is that the yield stress is not a well-defined term at high temperature due to its dependence on the loading condition. In other words, yield stress is not a material property. The applicability of classicial rate-independent plasticity theory, in which the concept of yield stress is essential, to describe the deformation at high temperature is therefore questionable.

Secondly, following the proposal by Rice (9), the above rate-sensitive yielding can actually be interpreted as a reflection of the role of the time-dependent strain (or creep strain). If the loading rate is high, the time-dependent strain does not have enough time to develop during loading, a well-defined elastic region may be found. When the loading rate gets lower, this elastic region should gradually diminish due to the involvement of the time-dependent strain. When the materials reach the steady state, the time-dependent strain rate at a particular stress level is fixed. In a constant strain rate test, when the stress is increased to a level in which the time-dependent strain rate is equal to the imposed strain rate, the stress will stay constant. At room temperature, the creep rate of most structural materials is so low that the stress-strain curve based on loading times of order of minutes does not differ significantly from those based on seconds, hours, or days. This may be considered as a limiting case for which the rate-independent plasticity theory could be applied.

Based on the above discussion, we may conclude that at high temperature, all the materials are essentially rate-sensitive, i.e., time-dependent. The traditional definition of plastic strain and creep strain at high temperature based on material testing only refers to different macroscopic material behavior under different loading conditions, i.e., constant strain rate loading versus constant load loading. The "instantaneous" response has no meaning unless the loading rate (or strain rate) is specified. Consequently, there seems no physical background to study the so-called creep-plasticity interaction. In fact, when the steady state is reached, both load and strain rate are constant. There is even no distinction between creep test and constant strain rate test any more.

Modeling of the Experimental Results

In the previous work (4-7), a viscous-viscoelastic model was developed to model the experimental results of creep under variable biaxial loadings. The material constants were determined by quite a few creep and creep recovery tests. As mentioned earlier, since there exist some variations in the mechanical properties between the specimens in the current study and those in previous work no attempts was made to use previous theoretical model to predict the current experimental results or to redetermine the material constants due to the limited amount of specimen. Instead, some other constitutive equations were considered.

Due to its simplicity, the constitutive equation proposed by Bodner (10) and Mertzer (11,12) were tried to model the current experimental results.

For uniaxial stress state, the constitutive equation can be stated as follows:

$$\dot{\varepsilon}^P = \frac{2D_o}{\sqrt{3}} \left(\frac{\sigma}{|\sigma|}\right) \exp\left[-(1/2)(z^2/\sigma^2)^n\right] \tag{1}$$

and

$$\dot{z} = m(z_1 - z)\sigma\dot{\varepsilon}^P - A(z - z_o)^q \tag{2}$$

where $\dot{\varepsilon}^P$ is the inelastic strain rate, σ is the applied stress, z is a scalar state variable whose initial value and the saturation value are z_o and z_1 respectively, and is assumed to be a function of plastic work. D_o, n, m, A, q are the material constants. As shown in eqn. (2), the rate of change of $z(\dot{z})$ is governed by work-hardening, $m(z_1 - z)\sigma\dot{\varepsilon}^P$, and softening due to thermal recovery, $A(z - z_o)^q$.

As shown in the paper by Merzer and Bodner (11), if neglecting the recovery term, the above constitutive equation can be integrated to get an explicit stress-plastic strain relation for the case when the plastic strain rate is constant. The assumption of constant plastic strain rate can actually be applied to the later stages of the three curves shown in figure 6 because the stress increment and thus the elastic strain increment, is almost zero.

By fitting the integrated equation to these three curves, the material parameters used in equations (1) and (2) can be determined for the current material. The values of these constants are: D_o: 10^4 sec^{-1}; n: 0.79; m: 19.0 MPa^{-1}; z_o: 525 MPa; z_1: 1092 MPa. The theoretical results are shown in figures 1(b), 2(b), and 3(b) as dotted lines. Because equations (1) and (2) was for uniaxial stress state, no theoretical predictions was made for the data shown in figure 5.

Discussion of The Theoretical Model

The theoretical results shown in figures 1(b) and 2(b) showed some discrepancies with the experimental data. Furthermore, the predicted steady state stress at each step in figure 1(b) is almost the same as that at the corresponding step in figure 2(b) with the same imposed strain rate, respectively. This was found to be due to the fact that in both cases the scalar state variable z almost reached its saturation value z_1 at the end of the first step and stayed there for the whole test. With a constant value of z, a unique stress should of course be expected for a specified strain rate.

When equations (1) and (2) are applied to the creep test, figure 3, it can be seen that the general trend of the material behavior seems satisfactorily described especially for the transient response at the first loading step. The results could be improved by including the thermal recovery term which seems quite important in the low strain rate tests. However, the current experimental information is not enough for identifying this term.

Based on the above results, it seems reasonable to conclude that constitutive equations based on the data from constant strain rate material testing should be able to predict the material behavior in a constant load creep test or vice versa, i.e., a unified equation should work well for various kinds of loadings. However, there is one very important point which needs to be clarified here. In the current tests, all the constant strain rate tests were performed at the strain rates which are comparable to those during a constant load creep test, namely 10^{-9}/sec to 10^{-6}/sec. However, the strain rates usually used in the study of plasticity, e.g., creep-plasticity interaction, are in the range from 10^{-5}/sec to 10^{-2}/sec which are generally available in a commercial testing machine. In this case, the constitutive equation derived from the data from creep tests may not be able to predict the material behavior during a constant strain rate tests because of different ranges of strain rates involved. Therefore, it seems important to keep in mind that in order to develop a unified constitutive equation which can interpret the traditional creep-plasticity interaction, test data covering a wide range of strain rates seems necessary.

Conclusions

Metals are essentially rate sensitive at elevated temperatures. The traditional definition of creep and plasticity used in the classical creep analysis is actually a reflection of the material behavior under different loading conditions. A unified constitutive equation should work well for various kinds of loading conditions as long as the strain rates are comparable to each other.

Acknowledgement

This study was supported in part by funds provided by Washington State University and the National Science Foundation under Grant No. MEA-84029. The authors are grateful to Prof. W.N. Findley (Division of Engineering, Brown University) for helpful discussions. Thanks are also due to Ms. Jo Ann Rattey for typing the manuscript.

References

1. Pugh, C.E., "Progress in developing constitutive equations for inelastic analysis," J. of Pressure Vessel Tech., 105, 273-276, 1983.

2. Kraus, H., Creep Analysis, Wiley, New York, 1980.

3. Ohashi, Y., Kawai, M., and Shimizu, H., "Effects of prior creep on subsequent plasticity of Type 316 stainless steel at elevated temperature," ASME J. Eng. Mat'ls and Tech., 105, 257-273, 1983.

4. Ding, J.L. and Findley, W.N., 1984a, "48 Hour multiaxial creep and creep recovery of 2618 aluminum alloy at 200°C," ASME J. of Appl. Mech., 51, 125-132.

5. Ding, J.L. and Findley, W.N., 1984b, "Multiaxial creep of 2618 aluminum under proportional loading steps," ASME J. Appl. Mech., 51, 133-140.

6. Ding, J.L. and Findley, W.N., 1985, "Nonproportional loading steps in multiaxial creep of 2618 aluminum," ASME J. of Appl. Mech., 52, 621-628.

7. Ding, J.L. and Findley, W.N., 1986, "Simultaneous and mixed stress relaxation in tension and creep in torsion of 2618 aluminum," ASME J. Appl. Mech. (to appear).

8. Findley, W.N. and Gjelsvik, A., "A biaxial testing machine for plasticity, creep or relaxation under variable principal stress ratios," Proceedings, ASTM, 62, 1103-1118, 1962.

9. Rice, J.R., "on the structure of stress-strain relations for time-dependent plastic deformation in metals," ASME J. Appl. Mech., 728-737, 1970.

10. Bodner, S.R. and Partom, Y., "Constitutive equations for elastic-viscoplastic strain hardening materials," ASME J. Appl. Mech., 42, 385-389.

11. Merzer, A.M. and Bodner, S.R., "Analytical formulation of a rate and temperature dependent stress-strain relation," ASME J. of Eng. Mat'l Tech., 101, 254-257.

12. Merzer, A.M., "Steady and transient creep behavior based on unified constitutive equations," ASME J. of Eng. Mat'l Tech., 104, 18-25.

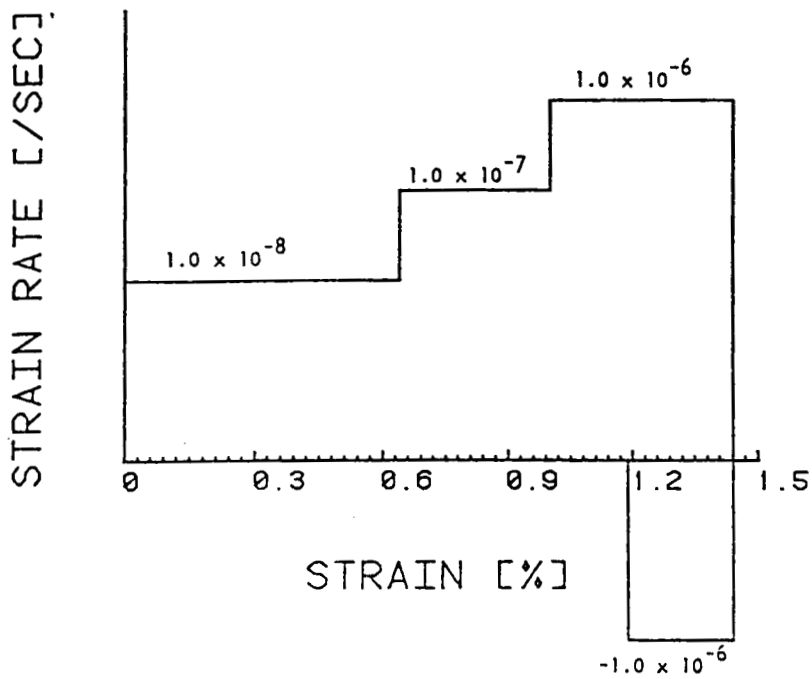

Figure 1(a): Loading program for a controlled strain rate test under stepwise increased strain rates.

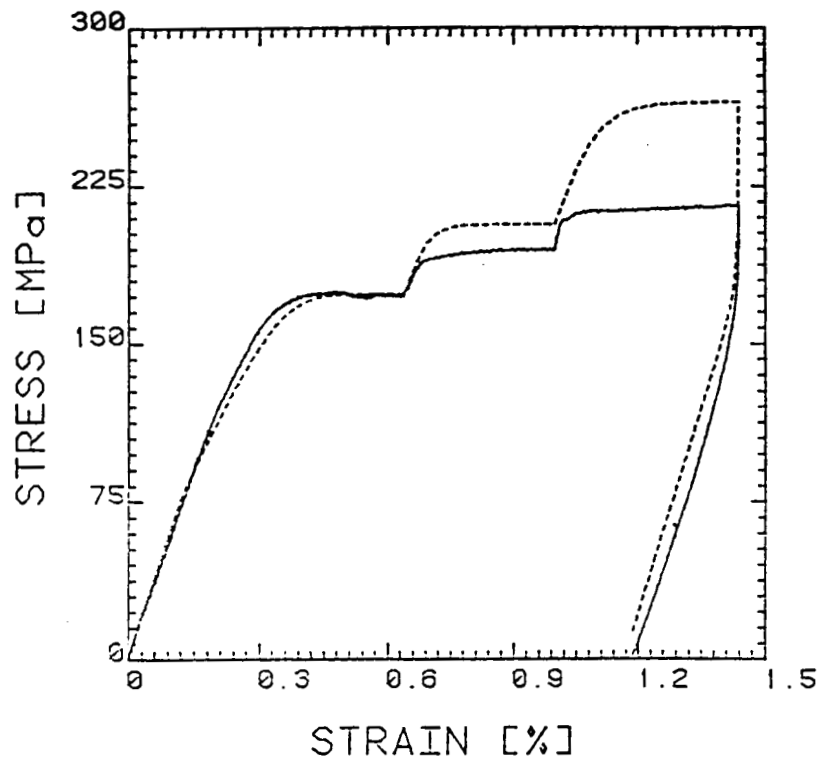

Figure 1(b): Experimental (solid lines) and theoretical (dotted lines) results for the loading program shown in figure 1(a).

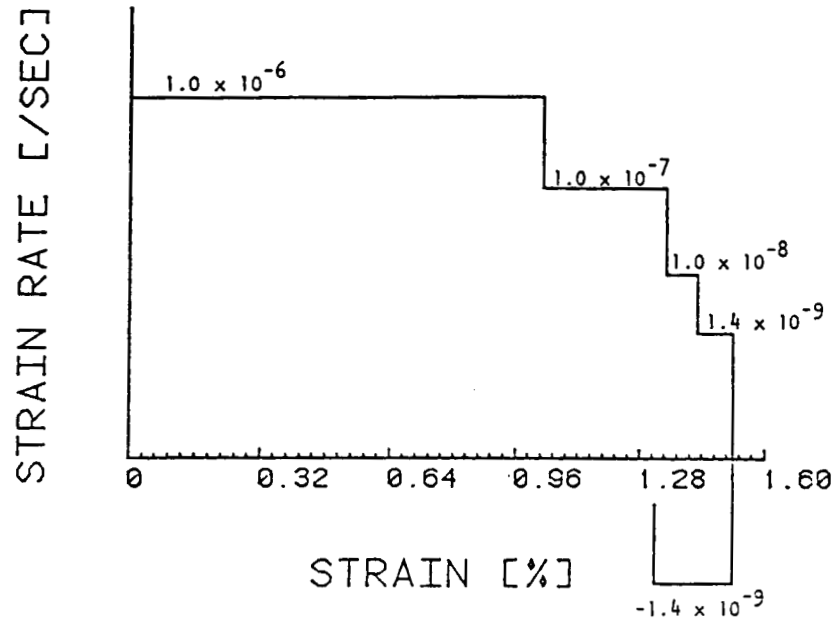

Figure 2(a): Loading program for a controlled strain rate test under stepwise decreased strain rates.

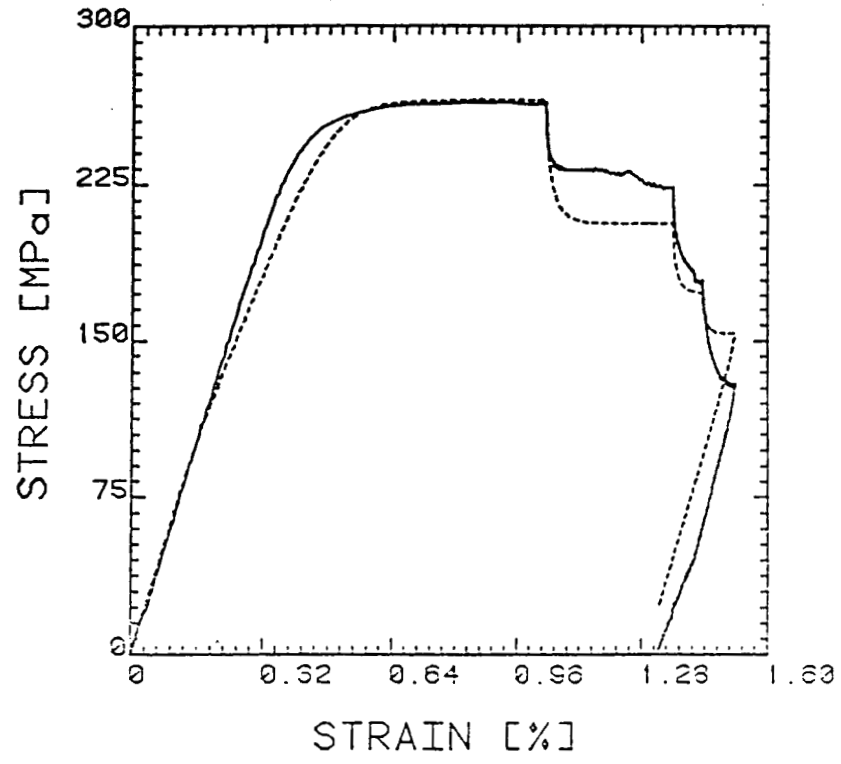

Figure 2(b): Experimental (solid lines) and theoretical (dotted lines) results for the loading program shown in figure 2(a).

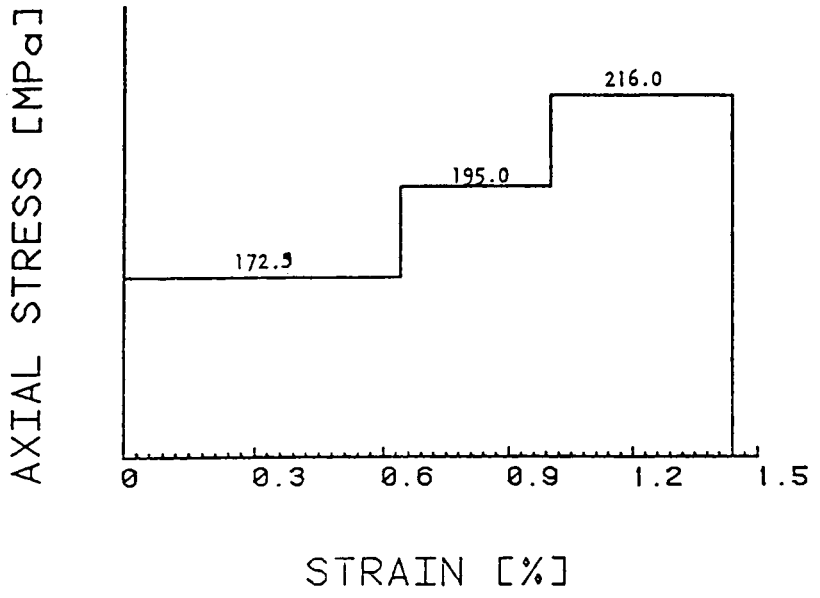

Figure 3(a): Loading program for a creep test under stepwise increased stresses. The stress at each step is equal to the steady state stress at the corresponding step in figure 1(b), respectively.

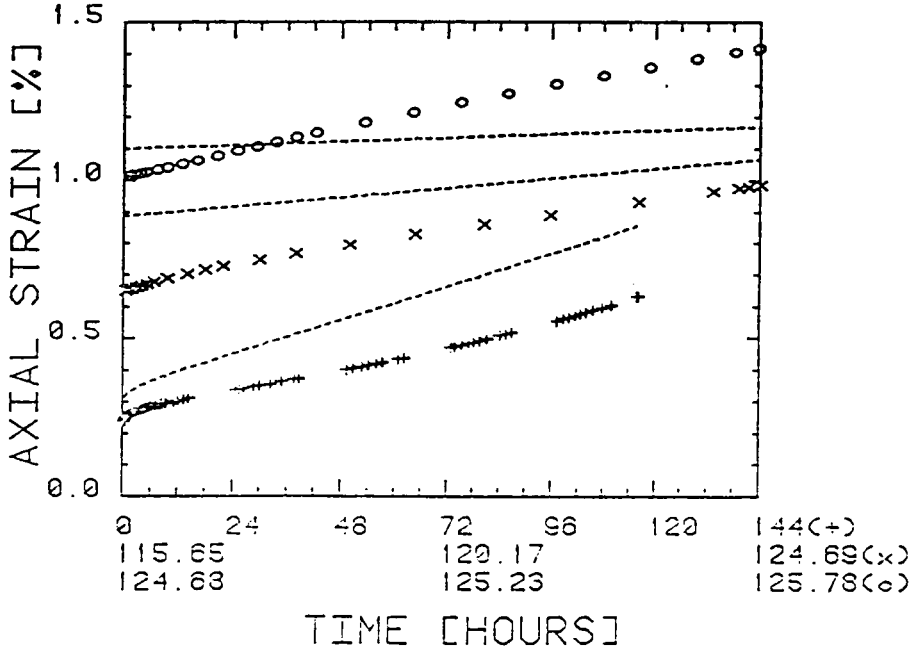

Figure 3(b): Experimental (solid lines) and theoretical (dotted lines) results for the loading program shown in figure 3(a). Notice that different time scales were used for each step.

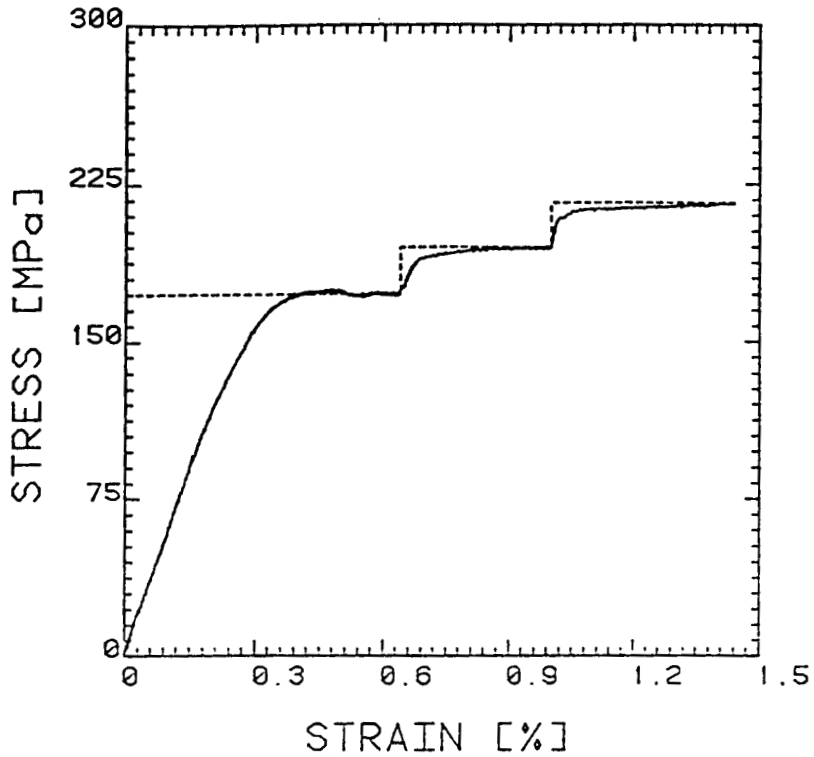

Figure 4(a): Comparison of the results in figure 1(b) and figure 3(a) in terms of stress and strain. Solid lines are the results of constant strain rate test, while dotted lines are the loading program for creep test.

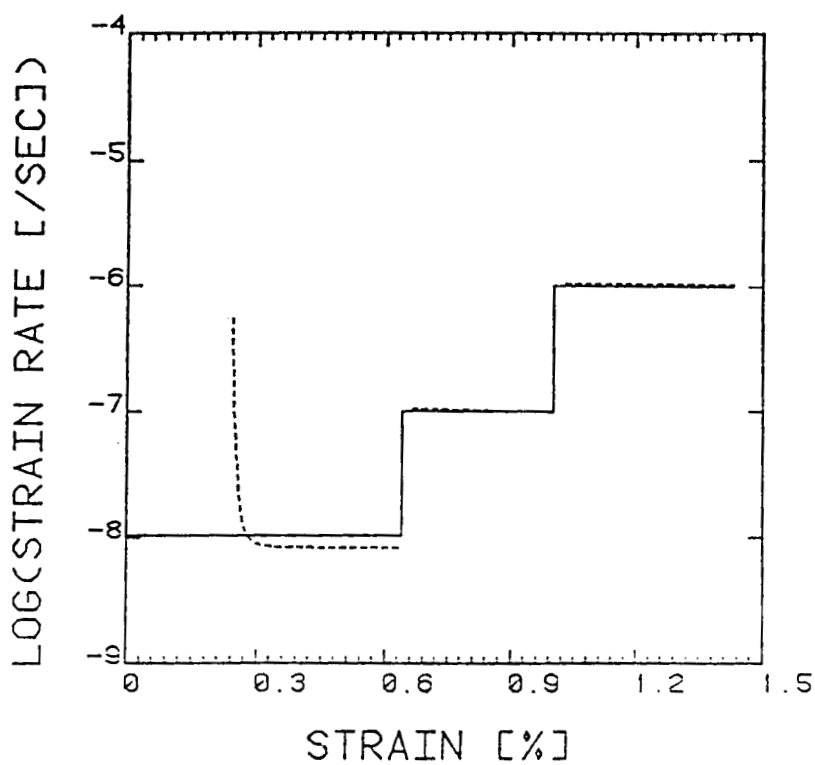

Figure 4(b): Comparison of the results in figure 1(a) and figure 3(b) in terms of strain rate and strain. Solid lines are the loading program for constant strain rate tests, while dashed lines are the results of creep tests.

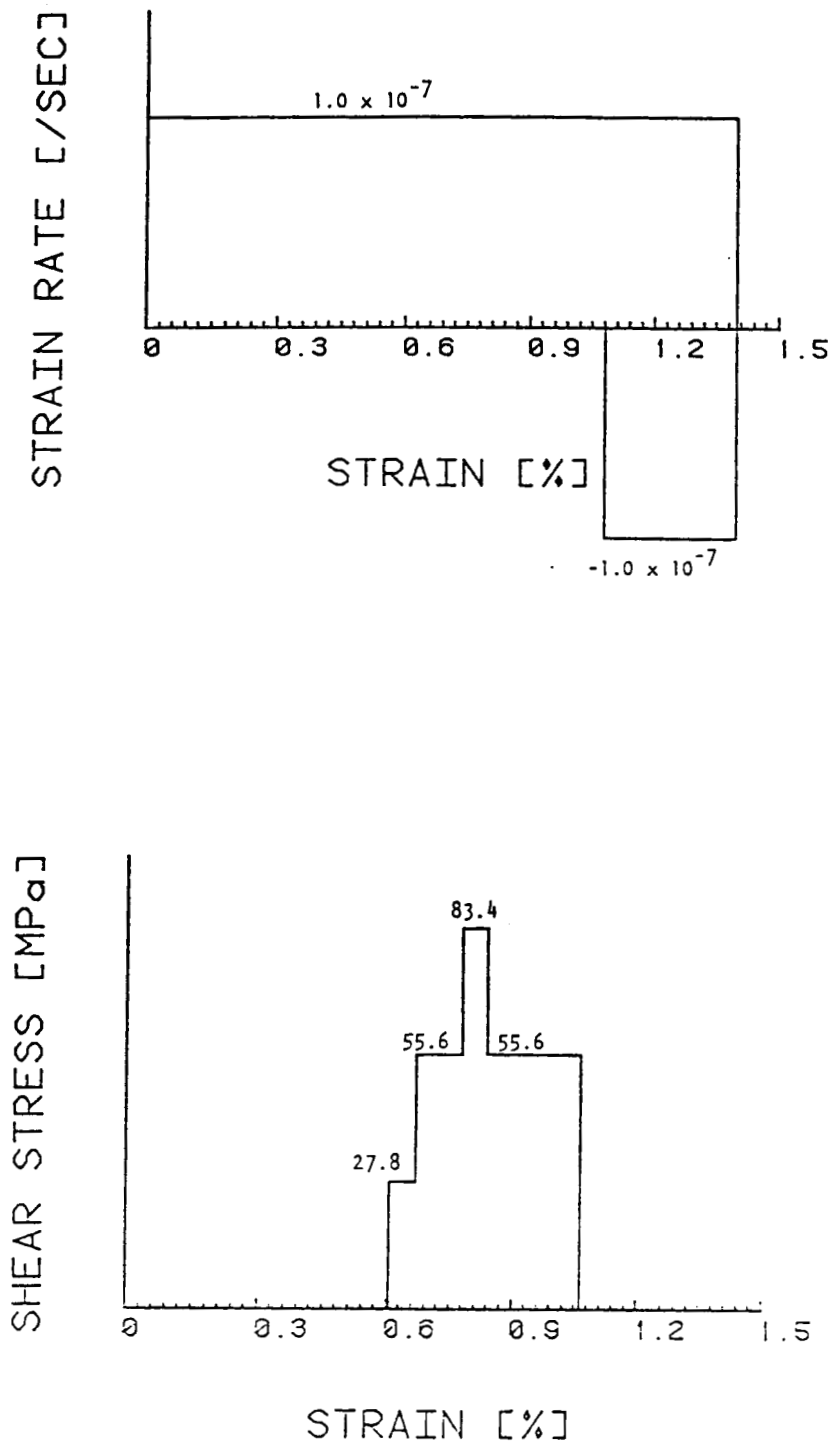

Figure 5(a): Loading program for a test under constant-strain-rate axial loading combined with stepwise varied torsional loadings.

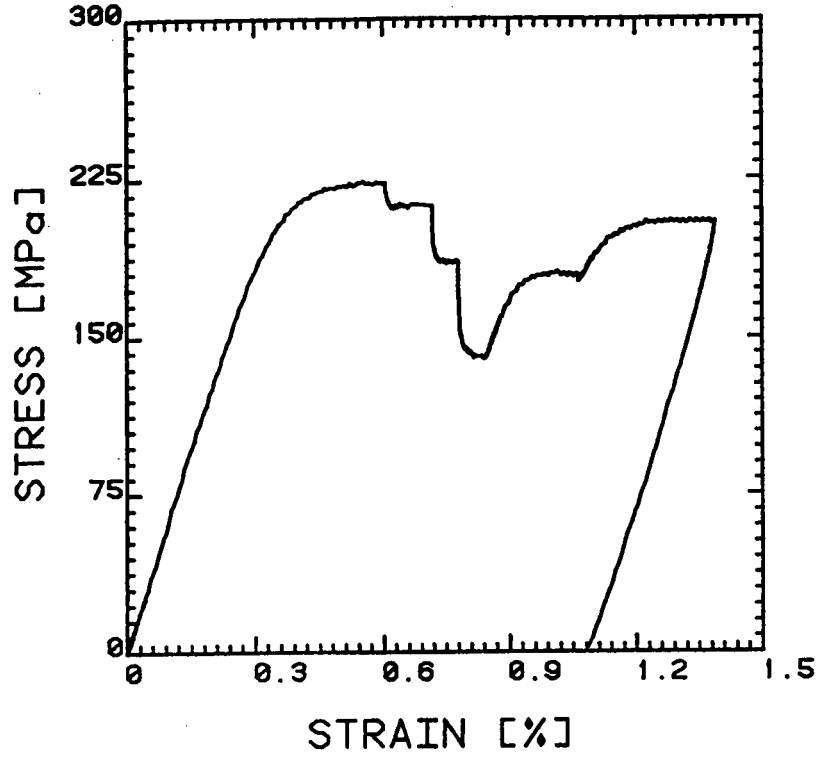

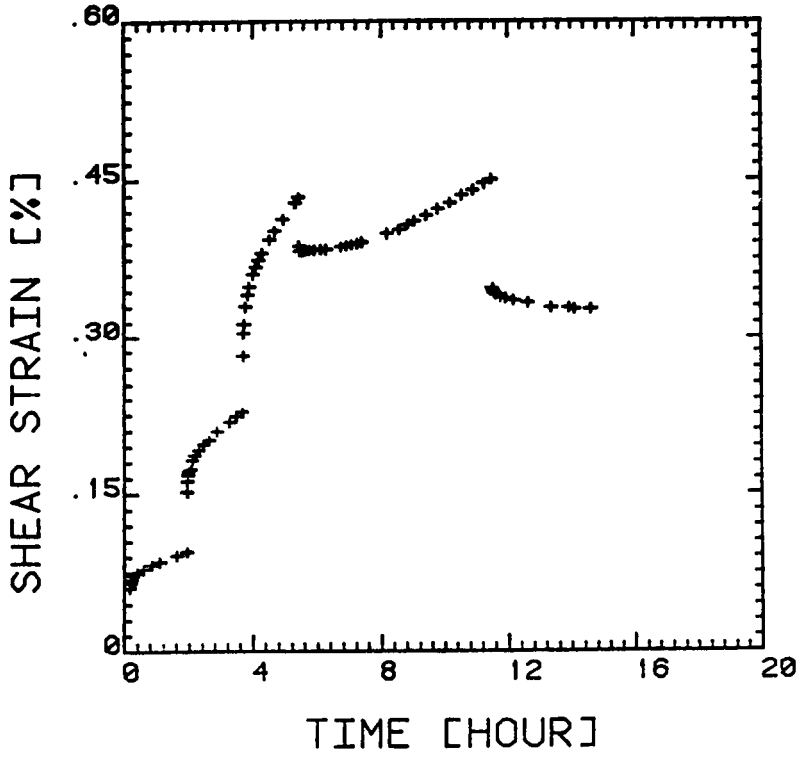

Figure 5(b): Experimental results for the loading programs shown in figure 5(a).

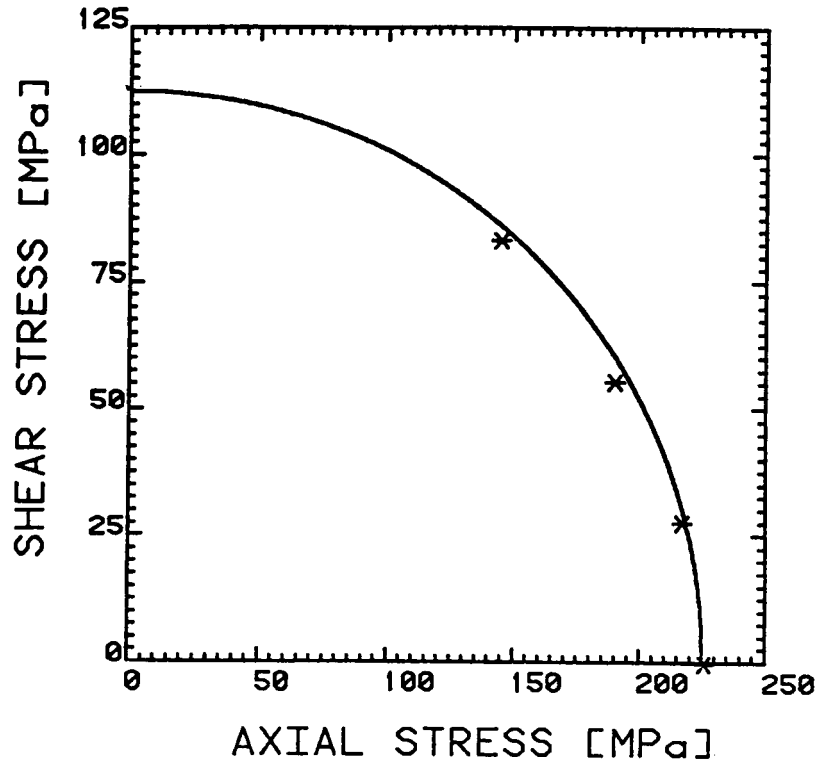

Figure 5(c): Stresses at steady states for steps 2, 3, and 4 shown in a two-dimensional stress space. The solid line is the Tresca curve.

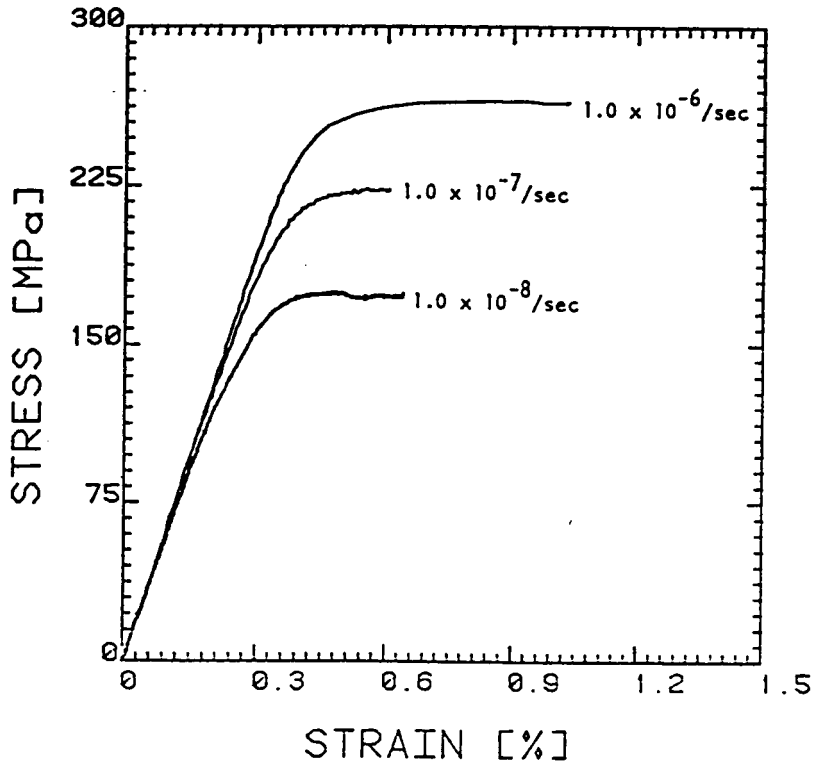

Figure 6: Stress-strain relations at different strain rates.